Iconic-Geometric Nonlinear Registration of a Basal Ganglia Atlas for Deep Brain Stimulation Planning

Ana B. Graciano Fouquier, Stanley Durrleman, Jérôme Yelnik, Sara Fernández-Vidal, Eric Bardinet

Iconic-Geometric Nonlinear Registration of a Basal Ganglia Atlas for Deep Brain Stimulation Planning

Ana B. Graciano Fouquier[1,2,3], Stanley Durrleman[1,2,3], Jérôme Yelnik[1], Sara Fernández-Vidal[1,2,4], and Eric Bardinet[1,2,5]

[1] Sorbonne Universités, UPMC Univ Paris 06 UMR S 1127, and Inserm U 1127, and CNRS UMR 7225, and ICM, F-75013, Paris, France
[2] Inria Paris-Rocquencourt
[3] ARAMIS Team
ana.fouquier@icm-institute.org, stanley.durrleman@inria.fr
[4] STIM Platform (Stereotaxy : Techniques, Images and Models)
sara.fernandez_vidal@upmc.fr
[5] CEnter for Neuro-Imagery Research - CENIR
eric.bardinet@upmc.fr

Abstract. This paper evaluates a nonlinear registration method for warping a 3D histological atlas of the basal ganglia into patient data for deep brain stimulation (DBS) planning. The power of the method is the possibility to combine iconic registration with geometric constraints under a unified diffeomorphic framework. This combination aims to ensure robust and accurate atlas-to-patient warping and anatomy-preserving deformations of stimulation target nuclei. A comparison of the method with a state-of-the-art diffeomorphic registration algorithm reveals how each approach deforms low-contrasted image regions where DBS target nuclei often lie. The technique is applied to T1-weighted magnetic resonance images from a cohort of Parkinsonian subjects, including subjects with standard-size and large ventricles. Results illustrate the effects of iconic or geometric registration alone, as well as how both constraints can be integrated in order to contribute for registration precision enhancement.

Keywords: nonlinear registration, diffeomorphism, basal ganglia, subthalamic nucleus, Parkinson's disease, deep brain stimulation

1 Introduction

In deep brain stimulation surgical planning, targeting of the basal ganglia is an important step, since it allows to estimate the location of target nuclei in the patient's brain. These estimates are used to plan the possible trajectories for electrode implantation during surgery. Precise positioning of electrodes is a key factor for the success of DBS, since stimulation of areas surrounding the target nuclei instead of the nuclei themselves, or stimulation of distinct territories within the same target, such as the motor or limbic parts of the subthalamic nucleus (STN), may account for drastic negative side-effects [1–3].

Automatic atlas registration methods are among the solutions [4–6] for anatomical targeting. These methods usually depend on the data to be registered, on a transformation model of the possible deformations (rigid, affine, nonlinear), and on a similarity measure to align atlas and patient data. The suitability of each transformation type and similarity criterion depends on the problem at stake. A registration method suitable for DBS applications should be able to map a basal ganglia atlas to a patient's brain robustly and accurately, while respecting anatomical constraints. For example, although inter-subject variability of subcortical structures is natural, these structures may share common shape patterns that are not expected to change significantly unless a pathology induces such deformations. However, targeting of DBS nuclei in images may be difficult, since certain nuclei (e.g. STN) are hardly or only partially visible in 1.5T T1 or T2-weighted magnetic resonance images (MRI). In these cases, the estimation of target nuclei location must rely on their surrounding visible structures.

This paper evaluates a nonlinear registration algorithm applied to the problem of atlas-to-patient basal ganglia registration of 1.5T T1-weighted MRI from DBS-eligible patients treated in the local neurosurgical department. This new method aims at improving, by means of nonlinear deformations, the accuracy of the current two-step rigid/affine registration, which is not always capable of satisfactorily registering the atlas data to the patient brain, especially in the case of subjects with large ventricles. This deformation model introduces a unified formalism for the use of geometric and iconic constraints. Iconic information is often considered when aligning image contours that are present everywhere in the image domain. Also, labeled structures segmented from images and represented by geometric entities (e.g. 3D surface meshes) may be used as geometric constraints. However, geometric registration is defined only on the contours to be aligned, and does not cover the whole image domain as in the iconic case.

The main advantage of the unified approach is thus the possibility to combine iconic and geometric information, since geometry can be used as a constraint to guide local anatomical deformations, whereas the intensity-based information can account for deformations in other regions. This combination is attained by choosing a suitable deformation defined in the ambient space (the domain embedding images and surfaces to be registered), which is also applicable to every object embedded in such a space. This is possible because the parametrization of deformations is made independent of the data to be registered. Our experiments show how each of these constraints alone influences registration, as well as how they can be put together to improve atlas-to-patient warping. Results also show that the modeled class of diffeomorphisms produces desirable anatomy-preserving deformations of the subthalamic nucleus, unlike other nonlinear state-of-the-art methods.

2 Iconic-Geometric Diffeomorphic Nonlinear Registration

Consider a total of N_{obj} deformable objects (e.g. images, surfaces). Let S_k, $k = 1 \dots N_{obj}$, be a source object to be registered to a target object T_k, and let

M_k be its corresponding deformed object. Our purpose is to find a compound registration from these sources to their respective targets. Such a registration corresponds to a single diffeomorphic transformation $\phi^{c,\alpha}$ of the whole 3D space embedding all these objects, which is obtained thanks to the control point formulation introduced in [7] for geometric entities (curves, surfaces, etc.)[6] and in [8] for images. The proposed formalism is built on these works and unifies the geometric and iconic diffeomorphic registrations under a single model.

Diffeomorphic deformations of all points in the ambient space are obtained through the integration of a time-varying vector field over the time interval $[0,1]$, given by $v_t(x) = \sum_i^{N_C} K(x, c_i(t))\alpha_i(t)$. Each α_i is a momentum vector associated to a control point c_i out of a total of N_C control points. These control points are not defined over the input data, but they are optimized within the ambient space and tend to move towards the most variable parts of the data. The previous equation defines a parametrization of diffeomorphisms that depends on the interpolation of the set of momenta located at the control points. It also describes the velocity of any point in the ambient space x at time $t \in [0,1]$. K is an interpolation Gaussian kernel that defines a Reproducing Kernel Hilbert Space (RKHS) and is given by $K(x,y) = \exp^{(-||x-y||^2)/\sigma_g^2}$. This shows that the deformation integrates iconic and geometric information contained in a neighborhood of size $\sigma_g \in \Re$, whereas points farther than σ_g from image contours or surfaces almost do not move.

To compute the compound registration of the set of deformable objects, which corresponds to a diffeomorphic transformation of the ambient space, we need to estimate the position of these control points and associated momenta. Given an initial set c_0 of control points and their associated set α_0 of initial momenta, this registration is achieved by minimizing the following objective function:

$$E(c_0, \alpha_0) = (\sum_{k=1}^{N_{obj}} \frac{1}{2{\sigma_k}^2} D(\phi^{c,\alpha} * M_k, T_k)^2) + Reg(\phi^{c,\alpha}) \ , \tag{1}$$

where D is a similarity measure computed between each transformed source data and their corresponding target, and Reg is a regularity term defined over the diffeomorphic transformation $\phi^{c,\alpha}$. For more details on the diffeomorphism $\phi^{c,\alpha}$, the reader is referred to [7, 8].

The parameter $\sigma_k \in \Re$ is of great importance. It consists in a scalar trade-off value between fidelity-to-data and the regularity of the sought deformation. It also balances the relative importance of each iconic and geometric constraint among themselves. Besides this, the underlying parameter σ_g plays a crucial role in the interpolation of geometric and iconic information present in the ambient space, as discussed previously in this section. It also regulates the scale at which deformations are taken into account. A small kernel will tend to consider local variations, which may be desirable when trying to register refined anatomical details, whereas a larger kernel will promote more homogeneous deformations.

[6] This diffeomorphic registration of geometric objects is implemented in the software *Deformetrica*, publicly available at `http://www.deformetrica.org`

If S_k and T_k are images, the similarity measure D is based on the quadratic error to the local affine model proposed in [9], which is more robust to source and target contrast differences than whole-image measures such as the sum of squared differences. This distance is defined as:

$$D(\phi^{c,\alpha} * M_k, T_k)^2 = \int (\sigma_p^2(\phi^{c,\alpha} * M_k) - \frac{Corr(T_k, \phi^{c,\alpha} * M_k)_p^2}{\sigma_p^2(T_k)})\mathrm{d}p. \quad (2)$$

$Corr(I, J)$ is the local correlation between two given images I and J , defined over a symmetric and normalized window function $W : \Re^d \rightarrow \Re$. Let W_p be the window translation around a point p and let x be a point in the images domain. Then $Corr(I, J)$ is written as:

$$Corr(I, J)_p = \int W_p(x)(I(x) - \int W_p(x)I(x)\mathrm{d}x)(J(x) - \int W_p(x)J(x)\mathrm{d}x)\mathrm{d}x. \quad (3)$$

Besides, $\sigma_p^2(I)$ is the local variance of a given image I, written as:

$$\sigma_p^2(I) = Corr(I, I)_p. \quad (4)$$

If S_k and T_k represent geometric primitives, D is a point-correspondence-free distance on varifolds, which are the adopted mathematical representations of geometric deformable objects in this formulation. When M_k and T_k are surfaces represented by computer meshes, the similarity measure is written as:

$$D(\phi^{c,\alpha} * M_k, T_k)^2 = < \phi^{c,\alpha} * M_k, \phi^{c,\alpha} * M_k > + < T_k, T_k > -2 < \phi^{c,\alpha} * M_k, T_k > , \quad (5)$$

where the operator $< S, S' >$ represents the inner product of two given surfaces S and S' represented by computer meshes and defined as:

$$< S, S' > = \sum_s \sum_{s'} K_W(p_s, p_{s'}) \frac{(n_s^T n_{s'})^2}{|n_s||n_{s'}|}, \quad (6)$$

where s (resp. s') is the total number of mesh cells composing the surface, p_s and n_s (resp. $p_{s'}$ and $n_{s'}$) represent the centers and normals of the faces in S (resp. S'), and $|n_s|$ (resp. $|n_{s'}|$) is the area of each mesh cell. Finally, K_W is a Gaussian function with a fixed standard deviation σ_W.

3 Atlas-to-Patient Registration

In the local neurosurgical department, targeting of basal ganglia is currently achieved through atlas-to-patient registration. DBS-eligible patient data consists of pre-operative T1-weighted MRI acquired with a GE® 1.5T scanner. The adopted atlas was described in [4, 10] and consists in a detailed 3D histological model of the human basal ganglia, obtained through the co-registration of histological and T1-weighted MRI data from a post-mortem specimen, which may

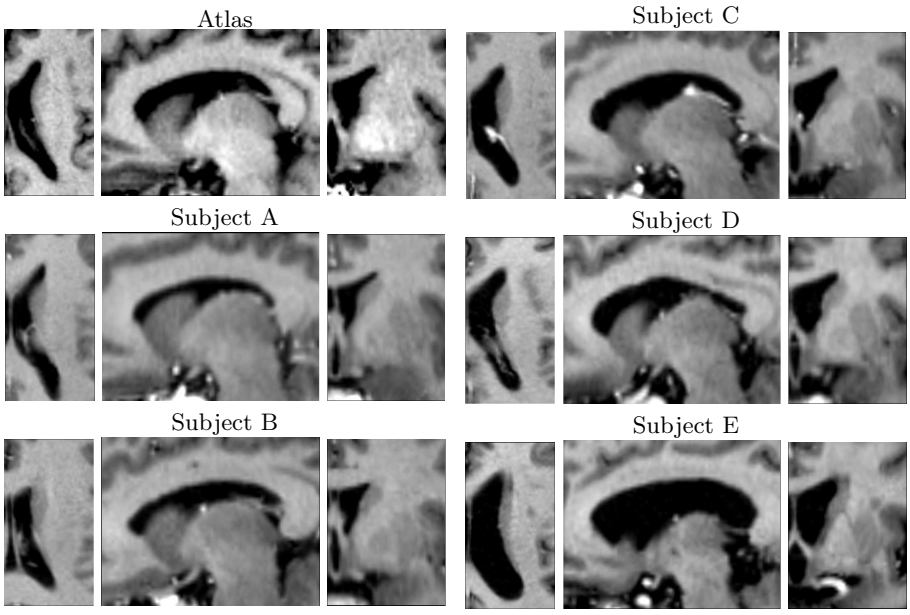

Fig. 1. Atlas left-hemispheric cropped volume from the post-mortem specimen MRI used in the registration process (top row, first three views to the left) and registered MRI left-hemispheric cropped volumes from five subjects of the local cohort of patients liable to DBS. For the atlas and for each subject, sample axial, sagittal, and coronal slices are shown from left to right.

be adapted into patient's space. Then, targeting of the basal ganglia follows a pipeline that is similar to the inclusion protocol described in [11]: first the AC-PC coordinates are interactively defined over the patient's MRI; then, the scalp, gray/white matter, and sulci are segmented from the T1-weighted MRI; finally, spatial normalization of the patient data in the atlas space is performed.

This normalization is achieved through a patient-to-atlas two-step image registration process. The patient's MRI is rigidly registered to the atlas MRI for brain volume alignment. Next, the result and the atlas image are cropped into two regions of interest (ROI) around the basal ganglia, resulting in right and left hemisphere ROIs. Finally, each hemispheric patient ROI is registered to the corresponding atlas ROI, through affine transforms, allowing for a more refined alignment of data around the basal ganglia. Examples of the atlas cropped volume and the registered input cropped volumes are shown in Fig. 1. All registrations are done with the Baladin software [10], a multiscale block-matching algorithm. Finally, the atlas meshes are deformed into the original patient MRI space by applying the composition of atlas-to-patient affine and rigid matrices to each mesh. This allows for easy assessment[7] of registration quality directly over the patient MRI. Although this pipeline is robust for STN targeting, the

[7] Results visualized with the software *3D Slicer* (`http://www.slicer.org`).

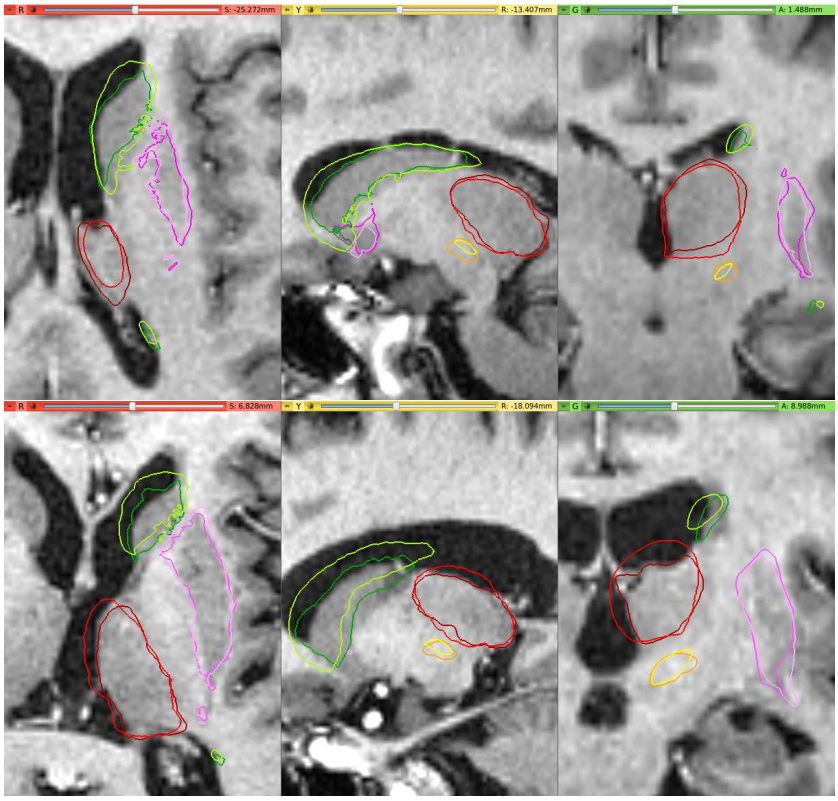

Fig. 2. Registration deformations obtained from the Baladin algorithm (brighter colors) and from ANTS with standard parameters (darkers colors), applied to meshes of the caudate nucleus (green), thalamus (red), putamen (pink), and subthalamic nucleus (yellow/orange). These meshes were warped into the image space of a subject D with standard-size ventricles (top) and a subject E with large ventricles (bottom). Although ANTS produces accurate caudate and thalamus registrations, its deformations implied onto the STN do not preserve anatomy.

rigid-affine combination is not always accurate for dealing with patient-to-atlas deformations that are of nonlinear nature. For instance, one common pitfall concerns the caudate nucleus, whose corresponding region tends to go over the actual ventricle region after registration, as seen in Fig. 2. This typical problem leads us to consider the adoption of a nonlinear registration step in the basal ganglia targeting pipeline.

Nonlinear registration methods may cope with broader types of deformations and, thus, produce more precise patient-to-atlas registration, but a common drawback is that they may also lead to spurious deformations due to image noise or to the way the deformation model acts in low-contrast image regions. For instance, the software ANTS [12, 13] accurately aligns anatomical structures

that present high contrast and are fairly visible in a given image, such as the caudate, the ventricles, and the thalamus. However, structures present in low-contrast image regions, e.g. the STN, are deformed in an unrealistic manner. This effect is shown in Fig. 2 for the STN, whose left-hemispheric 3D histological mesh was warped into patient space according to the deformation field found by ANTS for atlas-to-patient registration. In the ANTS deformation model, image forces computed in high-contrast regions propagate to low-contrast regions and dominate the deformation of the more homogeneous regions. Thus, the good accuracy in the alignment of highly-contrasted structures is done at the cost of less controlled deformations in low-contrast regions. On the other hand, the registration model proposed in Sect. 2 deals with low-contrasted and weak-gradient regions in a distinct manner. It tends to penalize deformations in such regions, leading to anatomy-preserving deformations of the STN. Next, we discuss the experimental assessment of this method.

3.1 Experimental Results

For these experiments, subcortical structures surfaces represented by meshes were obtained with the automatic subcortical segmentation procedure *recon-all* [14], from the *Freesurfer* image analysis suite, which provides reasonable segmentations. Although the 3D histological atlas meshes are available, we also extracted subcortical structures from the atlas MRI using this software, in order to register meshes with the same level of detail. We adopted the left hemispheric lateral ventricle and caudate provided by Freesurfer as geometric constraints for our tests. For atlas-to-patient registration assessment, we warped the 3D histological atlas meshes according to each resulting diffeomorphic deformation, and subsequently transformed them into the original patient MRI space in the same way as explained in Sect. 3. The method was tested on the registered cropped volumes from the five patients depicted in Fig. 1. For illustration purposes, here we only show results for subjects A, D, and E, who present thinner, similar and larger ventricles with respect to the atlas postmortem specimen.

Iconic Registration. Consider the atlas left-hemispheric ROI, and the affinely-registered left-hemispheric ROI obtained for a given patient, as explained in Sect. 3. This first experiment consisted in registering the atlas ROI to the patient's ROI, using $\sigma_g = 3$mm as the convolution parameter, and $\sigma_1 = 0.71$ for the image data-fidelity parameter. The Gaussian kernel is small enough to capture image deformations occurring within small image regions, whereas the data-fidelity term was chosen in a way as to give as much importance to the data as to the allowed regularity of the sought deformation.

Figure 3 depicts registration results for subject A, whose lateral ventricles are smaller than those from the postmortem specimen, subject D, whose ventricles are of standard-size, and subject E, whose lateral ventricles are much larger. In all three cases, there is an improvement in the caudate and the thalamus registrations in comparison with the Baladin results. The chosen parameters

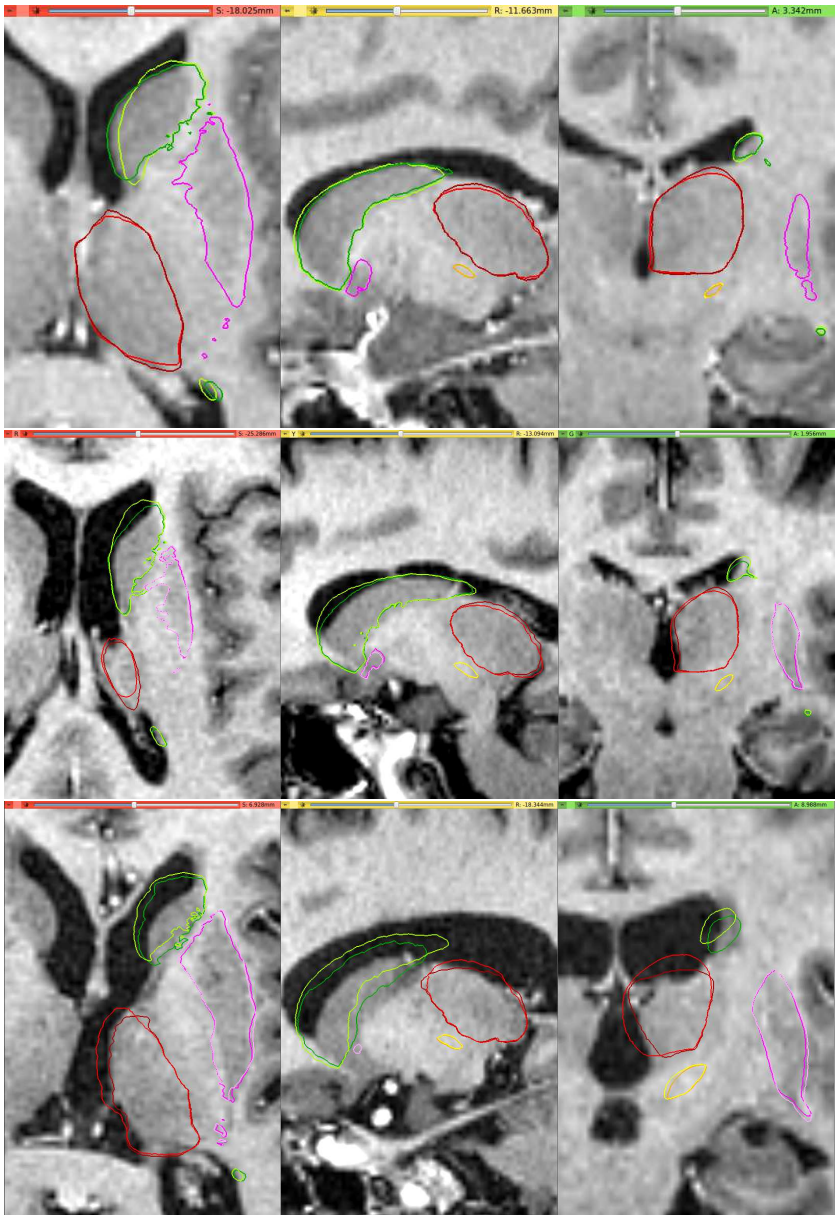

Fig. 3. Meshes warped according to our nonlinear registration using only iconic constraints (darker colors) and the Baladin algorithm (brighter colors) for subjects A (top), D (middle), and E (bottom). The color-structure correspondence is the same as that of Fig. 2 and will be consistently adopted throughout the paper. Although registration is enhanced in comparison with Baladin results, caudate accuracy still requires improvements, especially for subject E presenting large ventricles.

are suitable for obtaining a satisfying registration for subjects with standard-size ventricles. However, results are poorer for the subject with large ventricles, especially concerning the caudate-ventricle superposition. This is probably due to the size of σ_g, which is small in comparison with the ventricle or caudate differences between the atlas and this patient. In this case, the kernel K applied to each control point does not consider image gradients that are farther than σ_g and registration does not capture this large dissimilarity. Increasing the value of σ_g and/or adjusting the data-fidelity value could lead to better results.

Geometric Registration. This second experiment consisted in registering the atlas caudate mesh obtained from Freesurfer to the patient's respective Freesurfer mesh, using $\sigma_g = 3$mm, and $\sigma_1 = 0.71$ as the geometric data-fidelity parameter. Here, the sought diffeomorphism only considers geometric constraints. The caudate is the structure of choice, since it is one of the main structures whose registration must be improved. Figure 4 shows the results of the warpings of the atlas meshes according to the deformations found for the same subjects as before. In all three cases, the caudate-ventricle superposition problem is reduced with respect to the Baladin results. Also, atlas mesh alignment is improved for subjects D and E in comparison with the iconic case, even though the parameters are the same in both cases. However, the registration does not affect the whole thalamus, and this structure is only slightly enhanced. This is because geometric deformations decay exponentially as they move away from the surface mesh, according to the value of σ_g. Thus, they can only influence nearby regions, as it can be seen in the thalamus frontier close to the caudate in sagittal and coronal views.

Iconic-Geometric Registration. This last experiment consisted in registering simultaneously the atlas left lateral ventricle and caudate meshes obtained from Freesurfer, and its left hemispheric ROI to the patient's respective meshes and ROI. The adopted parameter values were $\sigma_g = 5$mm and $\sigma_1 = \sigma_2 = \sigma_3 = 0.1$. In this test, more importance was given to the geometric and iconic constraints with respect to the regularity term. The lateral ventricles and caudate nuclei were used as geometric constraints in the attempt to enhance registration for the subject with large ventricles. Results are illustrated in Fig. 5. Atlas mesh alignment for each basal ganglia structure is more precise in comparison with the iconic case and the results from Baladin. Unlike the purely geometric registration, improvements also occur in other image regions, such as in the thalami or putamen of these subjects since the iconic information also drives the registration.

4 Discussion

The results discussed in Sect. 3.1 show that our nonlinear diffeomorphic registration method is capable of improving atlas-to-patient registration where the current two-step rigid and affine combination presents drawbacks. The registration of the caudate was improved with respect to the accumbens area, and

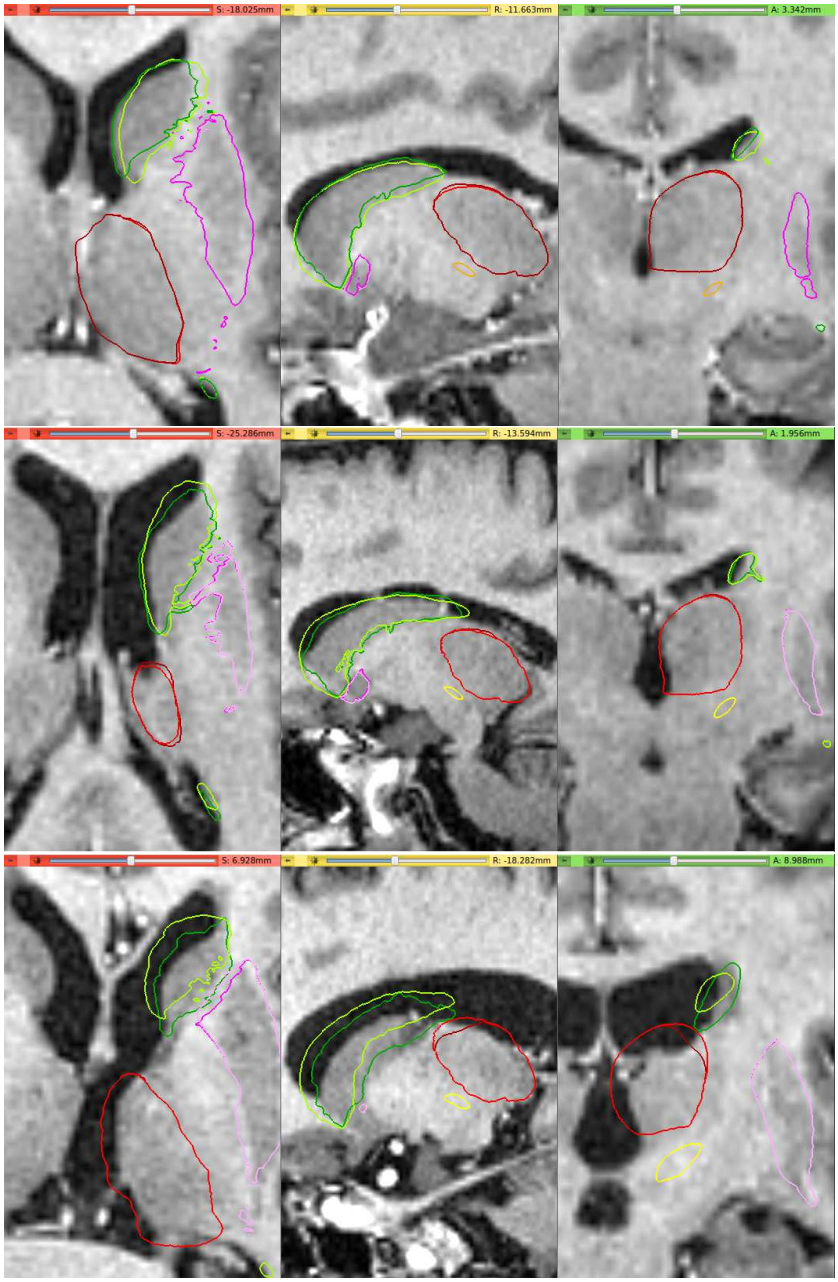

Fig. 4. Meshes warped according to our nonlinear registration using the caudate nuclei meshes as geometric constraints (darker colors) and the Baladin algorithm (brighter colors) for subjects A (top), D (middle) and E (bottom). Warping of the caudate is more accurate than in the iconic case for subjects D and E, but the underlying deformations do not affect other structures, especially those far from the adopted geometrical constraint.

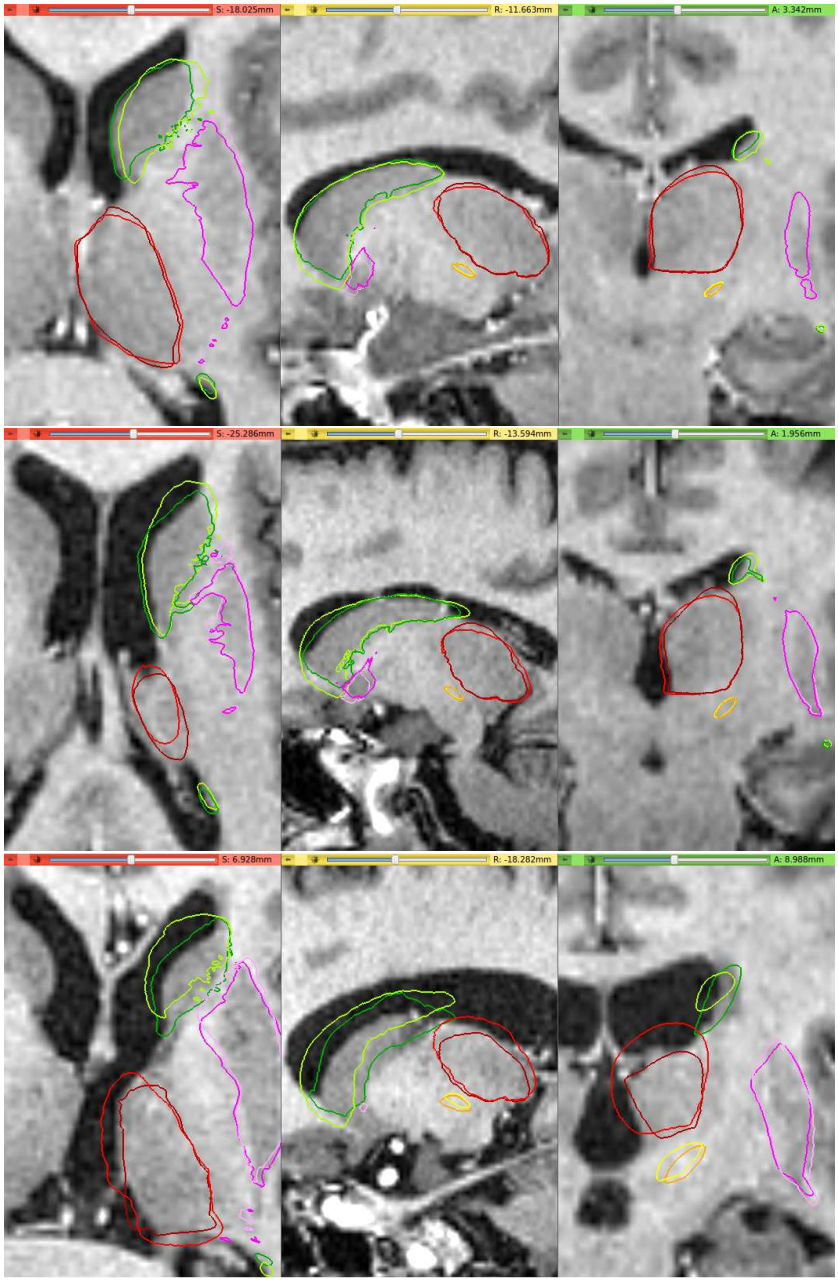

Fig. 5. Meshes warped according to our nonlinear registration using iconic and geometric constraints (darker colors), expressed by the lateral ventricles and caudate nuclei mesh, and the Baladin procedure (brighter colors) for subjects A (top), D (middle), and E (bottom). Caudate registration was enhanced for all subjects, while farther regions (e.g., the thalamus) were also deformed thanks to the iconic information simultaneously considered during the registration process.

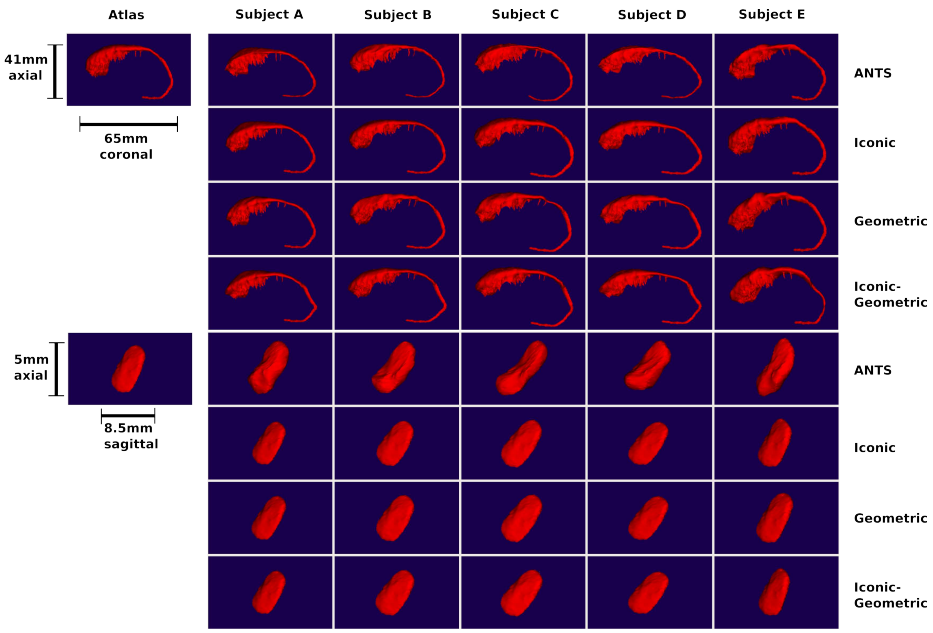

Fig. 6. Caudate and STN meshes deformed according to: ANTS, iconic information alone, geometric information alone, and combined iconic-geometric information for subjects A-E. The original atlas meshes are shown in the leftmost column as an anatomical reference. Meshes warped according to the deformations produced by our approach are more robust with respect to anatomy than those warped with ANTS.

ventricle-superposition was reduced in all three experiments. Thalamus registration was also enhanced. When merely geometric registration is considered, deformations impact only the regions surrounding the registered structure. To deform other regions in space, a set of geometric constraints covering various regions (e.g. thalamus, caudate, ventricle, putamen) should be registered simultaneously. On the other hand, the exclusive use of geometric constraints may also imply a dependence between registration quality and segmentation accuracy. If the input meshes come from successful segmentations, the geometric registration succeeds. Otherwise, it may fail.

This sensitivity to input mesh quality, as well as the global deformation issue, can be both dealt with by the iconic-geometric approach, since it allows the introduction of geometric constraints, while it still considers intensity cues. Thus, this solution benefits from both sources of information to improve atlas-to-patient registration as shown by our results. In this type of registration, the challenge is to choose the parameters corresponding to the data-fidelity term for each source of information in order to seize the best iconic-geometric compromise. Concerning parameters, the choice of σ_g is also crucial, because of its role in data interpolation and its direct influence in registration results.

In our qualitative comparative study, the experiments show that our non-linear registration method may be less accurate than ANTS in high-contrast regions, especially when using only iconic constraints, but the underlying diffeomorphic model better controls the impact of deformations in low-contrast regions, where the main DBS targets lie. Since the STN lies in such low-contrasted regions, warpings of the STN produced by our three diffeomorphic approaches (iconic, geometric, and iconic-geometric) respect the ovoid shape of this structure better than ANTS, as Fig. 6 shows[8]. On the other hand, ANTS registrations using the suggested default parameters produce less realistic shapes from an anatomical point of view. Even though structures such as the caudate are well-registered through ANTS, the STN is affected drastically by the resulting warpings. Tests with other combinations of ANTS registration parameters should be done to verify if anatomy could be preserved.

These fundamental differences are likely due to the distinct diffeomorphic deformation and regularity models adopted in ANTS and in our approach, as highlighted in Fig. 7. This figure presents the deformation fields obtained with ANTS registration for subject E, as well as with the three approaches discussed herein. These images show how each method deforms the original atlas cropped volume and its meshes according to the iconic and/or geometric information used. As a next step, we plan to perform a quantitative evaluation of the shape and location variations of the STN according to the deformations implied by the different registration approaches discussed herein.

Figure 8 depicts the STN meshes of subject E (large ventricles), warped according to ANTS, the iconic, geometric, and iconic-geometric approaches respectively, and superposed onto the T2 MRI corresponding to this subject. Because the STN and other targeted nuclei are not visible in 1.5T T1 MRI, we resorted to 1.5T T2 MRI images of the test subjects for a qualitative assessment of our registrations. These images may be used for visual inspection and estimation of the STN location [15], since it is partially visible as a hypo-intense signal, and surrounding nuclei, such as the red nucleus or the substantia nigra, are also visible and can be used as a visual guide for the STN location. Note that, despite this visibility, the STN structure cannot be completely defined from T2 MRI alone, since these images are not anatomical, thus requiring other sources of information (such as the T1-MRI atlas-based registration, electrophysiological recordings) to achieve satisfactory targeting. One can verify that the ANTS warping distorts the STN structure and increases it in the anteroposterior and axial axes (sagittal view), which is not desirable. It also moves the STN slightly into the substantia nigra (coronal view). The geometric registration produces a warping that almost does not change the original mesh adapted according to the Baladin registration transformation. This result is explained by the reasons we evoked previously in Sect. 3.1. Finally, the iconic and the iconic-geometric warpings show that the STN moves towards its likely position.

[8] The *ShapePopulationViewer* (`http://www.nitrc.org/projects/shapepopviewer/`) extension for *3D Slicer* was used for visual comparison of the warped surfaces.

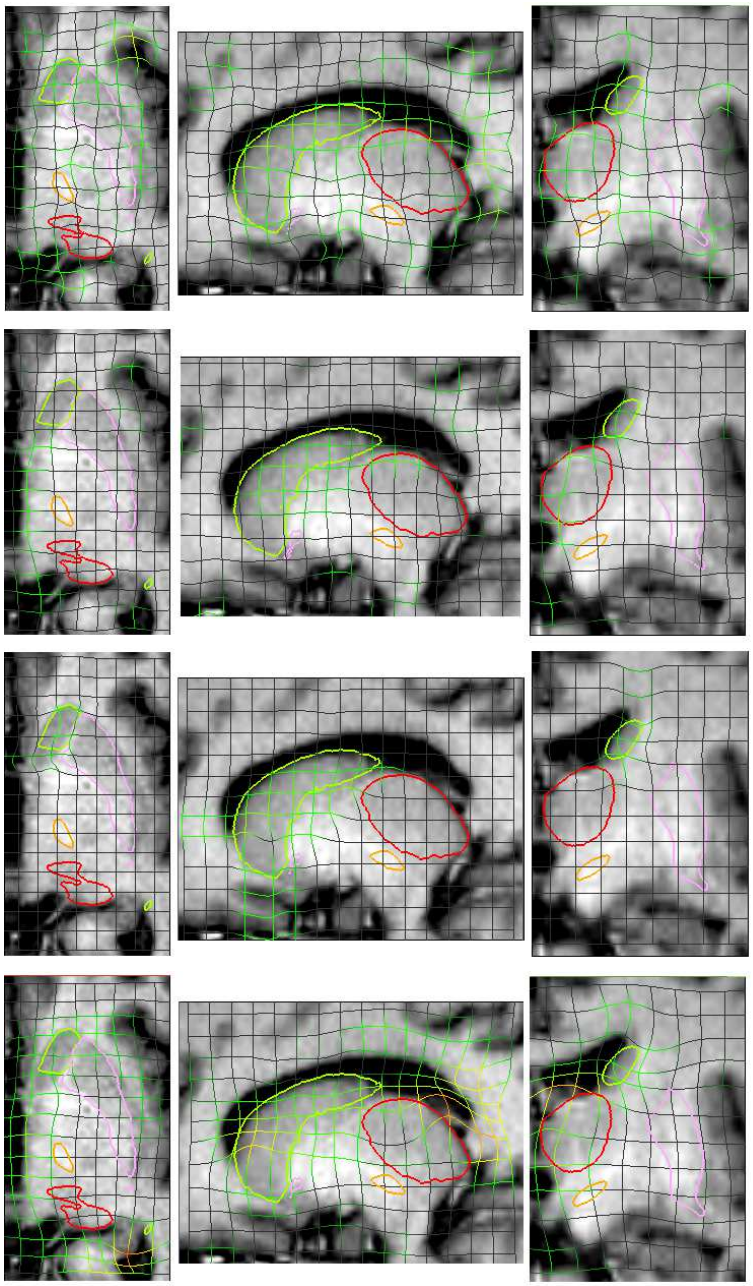

Fig. 7. Deformation fields produced by the registration of the atlas to subject E. Each field must be applied to the original atlas T1 MRI cropped volume and its corresponding meshes, shown in each row. For visualization purposes, the atlas STN is shown here in orange. From top to bottom: deformation field obtained using ANTS, iconic information alone, geometric information alone, and combined iconic-geometric information respectively. The low-contrasted image regions around the STN are less impacted by our three approaches than with ANTS.

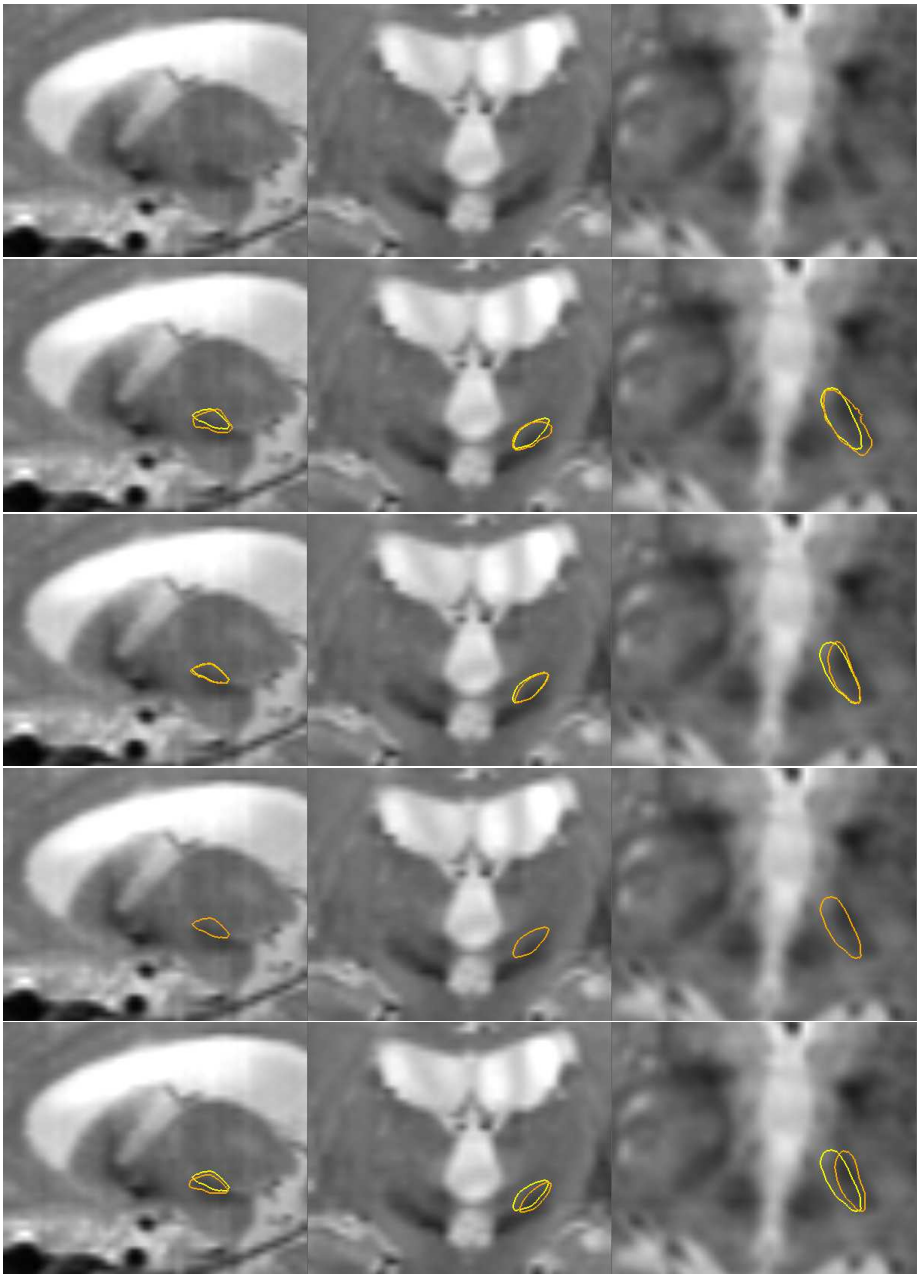

Fig. 8. Atlas STN meshes adapted according to the registration using Baladin (yellow) and warped according to the nonlinear registration algorithms (orange) superposed onto the 1.5T T2-MRI from subject E. From top to bottom: 1.5T T2-MRI slices (from left to right: sagittal, coronal, axial), and warped STN meshes obtained using ANTS, iconic information alone, geometric information alone, and combined iconic-geometric information respectively. Regions covered by ANTS-warped STN meshes overgo the STN regions, whereas our iconic and iconic-geometric approaches move it closer to the real STN position in the MRI.

All in all, we expect these improvements in atlas-to-patient registration precision to contribute for better surgical planning of the DBS electrode implantation trajectories to reach the targeted basal ganglia nuclei. This is particularly important, as the desirable location of electrode implantation becomes more and more refined, as it is the case of the STN and its limbic, sensorimotor and associative functional subterritories [3]. The higher precision alone cannot ensure the successful final outcome of DBS, since other possible sources of errors and imprecision may influence the pre-operative (e.g.: subcortical segmentation errors) and intra-operative procedures (e.g.: brain shift). Obviously, we believe that improving precision at each step of this complex process is an advisable practice. In this work, we focused on the accuracy improvement of the atlas-based targeting method. Although these preliminary results were obtained for a reduced cohort of patients, the respective data were representative of the broader population treated at the hospital, which encourages us to pursuit further testing and validation.

Acknowledgements. This research was partially funded by the program "Investissement d'Avenir ANR-10-AIHU-06" of the French Government. The authors would also like to thank the French Research Agency (ANR) for funding this study through the ACouStiC project (ANR 2010-BLAN-0209).

References

1. Groiss, S.J., Wojtecki, L., Südmeyer, M., Schnitzler, A.: Deep brain stimulation in parkinson's disease. Ther Adv Neurol Disord **2**(6) (2009) 20–8
2. Mallet, L., Schüpbach, M., N'Diaye, K., Remy, P., Bardinet, E., Czernecki, V., Welter, M.L., Pelissolo, A., Ruberg, M., Agid, Y., Yelnik, J.: Stimulation of subterritories of the subthalamic nucleus reveals its role in the integration of the emotional and motor aspects of behavior. Proc Nat'l Academy of Sciences **104**(25) (2007) 10661–10666
3. Welter, M.L., Schüpbach, M., Czernecki, V., Karachi, C., Fernández-Vidal, S., Golmard, J.L., Serra, G., Navarro, S., Welaratne, A., Hartmann, A., Mesnage, V., Pineau, F., Cornu, P., Pidoux, B., Worbe, Y., Zikos, P., Grabli, D., Galanaud, D., Bonnet, A.M., Belaid, H., Dormont, D., Vidailhet, M., Mallet, L., Houeto, J.L., Bardinet, E., Yelnik, J., Agid, Y.: Optimal target localization for subthalamic stimulation in patients with parkinson disease. Neurology (82) (2014) 1352–1361
4. Bardinet, E., Bhattacharjee, M., Dormont, D., Pidoux, B., Malandain, G., Schüpbach, M., Ayache, N., Cornu, P., Agid, Y., Yelnik, J.: A three-dimensional histological atlas of the human basal ganglia. II. Atlas deformation strategy and evaluation in deep brain stimulation for parkinson disease. J Neurosurg **110**(2) (2009) 208–19
5. Chakravarty, M., Sadikot, A.F., Germann, J., Hellier, P., Bertrand, G., Collins, D.L.: Comparison of piece-wise linear, linear, and nonlinear atlas-to-patient warping techniques: Analysis of the labeling of subcortical nuclei for functional neurosurgical applications. Hum Brain Mapping **30**(11) (2009) 3574–3595
6. Guo, T., Finnis, K.W., Deoni, S.C.L., Parrent, A.G., Peters, T.M.: Comparison of different targeting methods for subthalamic nucleus deep brain stimulation. In: Proc. Med Image Comput Computer Assist Interv. Volume 4190. (2006) 768–775

7. Durrleman, S., Prastawa, M., Charon, N., Korenberg, J.R., Joshi, S., Gerig, G., Trouvé, A.: Morphometry of anatomical shape complexes with dense deformations and sparse parameters. To appear in NeuroImage, **doi:10.1016/j.neuroimage.2014.06.043** (2014)
8. Durrleman, S., Allassonnière, S., Joshi, S.C.: Sparse adaptive parameterization of variability in image ensembles. Int J Comp Vision **101**(1) (2013) 161–183
9. Cachier, P., Bardinet, E., Dormont, D., Pennec, X., Ayache, N.: Iconic feature based nonrigid registration: The PASHA algorithm. Comp Vis Image Und **89**(2-3) (2003) 272–298
10. Yelnik, J., Bardinet, E., Dormont, D., Malandain, G., Ourselin, S., Tandé, D., Karachi, C., Ayache, N., Cornu, P., Agid, Y.: A three-dimensional, histological and deformable atlas of the human basal ganglia. I. Atlas construction based on immunohistochemical and MRI data. NeuroImage **34**(2) (January 2007) 618–38
11. D'Albis, T., Haegelen, C., Essert, C., Fernández-Vidal, S., Lalys, F., Jannin, P.: Pydbs: an automated image processing workflow for deep brain stimulation surgery. Int J Comput Assist Radiol Surg (2014)
12. Avants, B., Epstein, C., Grossman, M., Gee, J.: Symmetric diffeomorphic image registration with cross-correlation: Evaluating automated labeling of elderly and neurodegenerative brain. Med Image Anal **12**(1) (2008) 26 – 41
13. Klein, A., Andersson, J., Ardekani, Babak, A., Ashburner, J., Avants, B., Chiang, M.C., Christensen, Gary, E., Collins, D.L., Hellier, P., Song, J.H., Jenkinson, M., Lepage, C., Rueckert, D., Thompson, P., Vercauteren, T., Woods, Roger, P., Mann, John, J., Parsey, Ramin, V.: Evaluation of 14 nonlinear deformation algorithms applied to human brain MRI registration. NeuroImage **46**(3) (2009) 786–802
14. Fischl, B., Salat, D.H., Busa, E., Albert, M., Dieterich, M., Haselgrove, C., van der Kouwe, A., Killiany, R., Kennedy, D., Klaveness, S., Montillo, A., Makris, N., Rosen, B., Dale, A.M.: Whole brain segmentation: automated labeling of neuroanatomical structures in the human brain. Neuron **33** (2002) 341–355
15. Bejjani, B.P., Dormont, D., Pidoux, B., Yelnik, J., Damier, P., Arnulf, I., Bonnet, A.M., Marsault, C., Agid, Y., Philippon, J., Cornu, P.: Bilateral subthalamic stimulation for parkinson's disease by using three-dimensional stereotactic magnetic resonance imaging and electrophysiological guidance. J Neurosurg **92**(4) (2000) 615–625